crystals

*Article*

# Mechanical Properties of 6061 Aluminum Alloy under Cyclic Tensile Loading

**Tengjiao Hong [1,2], Fengjuan Ding [1,*], Feng Chen [1], Hua Zhang [1], Qiliang Zeng [1] and Juan Wang [1]**

[1] College of Mechanical Engineering, Anhui Science and Technology University, Fengyang 233100, China; hongtengjiao@ahstu.edu.cn (T.H.); chenf@ahstu.edu.cn (F.C.); zhangh@ahstu.edu.cn (H.Z.); zengql@ahstu.edu.cn (Q.Z.); wangjuan@ahstu.edu.cn (J.W.)
[2] School of Business Administration, Stamford International University, Bangkok 10250, Thailand
* Correspondence: dingfengjuan@ahstu.edu.cn; Tel.: +86-0550-6732037

**Abstract:** During the service process of an aluminum alloy structure, its complex deformation zone experiences repeated loading problems such as repeated tension, compression, bending and reverse bending. At the same time, the cyclic loading and heat treatment process also have a certain impact on the mechanical properties of aluminum alloy extruded tubes. Therefore, the study of heat treatment process parameters has important engineering and practical value for the mechanical properties of aluminum alloy extrusion tubes under cyclic loading conditions. The experiment takes 6061-T6 aluminum alloy extruded tubes as the research objects. In the study, heat treatment and cyclic tensile tests were carried out on 26 aluminum alloy specimens to study the effects of different heat treatment parameters (such as heating temperature, holding time, and cooling method) on the stress–strain hysteresis curves, stress characteristics, hysteretic energy, skeleton curves and failure characteristics of the alloy under the same loading system. In addition, different cyclic tensile tests were carried out on 20 aluminum alloy samples without secondary heat treatment to discuss the effects of different cyclic loading regimes on the mechanical properties of the alloy. The research results indicate that the effect of heating temperature on the cyclic loading performance of the alloy is greater than that of the holding time, and the effect of the cooling method on the cyclic loading performance of the alloy is not obvious. A cyclic tensile loading regime has a significant impact on the strength, elongation and hysteresis energy of the alloy. The hysteretic behavior of the alloy during cyclic tensile loading depends on the applied stress level and loading history. As the number of cycles increases, the shape of the hysteresis curve tends to be stable, but there is no monotonic relationship between the number of cycles loaded and the hysteresis energy.

**Keywords:** 6061 aluminum alloy extruded tube; cyclic tension experiment; hysteretic behavior; heat treatment process; stress control



**Citation:** Hong, T.; Ding, F.; Chen, F.; Zhang, H.; Zeng, Q.; Wang, J. Mechanical Properties of 6061 Aluminum Alloy under Cyclic Tensile Loading. *Crystals* **2023**, *13*, 1171. https://doi.org/10.3390/cryst13081171

Academic Editor: Shouxun Ji

Received: 12 July 2023
Revised: 21 July 2023
Accepted: 23 July 2023
Published: 27 July 2023



## 1. Introduction

During the use of an aluminum alloy construction, its complex deformation zone undergoes repeated loading problems such as repeated stretching, compression, bending and reverse bending. The uniaxial tensile test for aluminum alloy tubes is usually used to evaluate the mechanical properties and establish the constitutive model of the aluminum alloy tubes. However, the aluminum alloy material will have the characteristics of cyclic hardening, cyclic softening, the Bauschinger effect and cumulative damage of the material under cyclic loading, which makes the constitutive relationship of the materials very different under cyclic loading and monotonic loading. At the same time, the cyclic loading will also have a certain impact on the mechanical properties of aluminum alloy extruded pipes [1–3]. Therefore, it is of great practical value to study the mechanical properties of aluminum alloy pipes under cyclic loading.

At present, research on aluminum alloy components under cyclic loading mainly focuses on fatigue damage [4,5], fatigue life prediction [6–8], crack evolution [9–12], high/low cycle fatigue characteristics [13–16], etc. Research on aluminum alloy components or structures under cyclic loading is still limited. Byakov et al. [17] estimated the mechanical state of AA2024 tensile specimens based on Lamb wave ultrasonic technology, and their research results indicate that the signal characteristic parameters were dependent on the number of cycles during cyclic loading, and the behavior of these parameters is not linear. Pisapia et al. [18] conducted extensive experiments on 5000, 6000 and 7000 series aluminum alloys through monotonic and cyclic tests to obtain cyclic hardening, dissipated energy, plastic fracture and a nonlinear behavior of aluminum alloys. Ding et al. [19] conducted an experimental on the uniaxial cyclic deformation behavior of 6061-T6 aluminum alloy round bars at room temperature and high temperature. The results show that 6061-T6 aluminum alloy exhibits weak cyclic softening properties, and its ratcheting behavior depends not only on the mean stress and stress amplitude, but also on the loading history. Guo et al. [20] obtained the stress–strain relationship and hysteretic properties of domestic 6082-T6 and 7020-T6 aluminum alloys through cyclic loading tests. The research results show that aluminum alloy materials have good hysteretic properties and ductility. Zhao et al. [21] studied the stress cycling characteristics and hysteresis energy of AA6061, AA7075 and AA6063 aluminum alloys through repeated tensile tests. The results showed that the three alloys exhibit cyclic softening characteristics under repeated loading. Liu et al. [22] studied the effect of over-aging on the low-cycle fatigue behavior of an extruded AA6061 aluminum alloy at different strain amplitudes. The results showed that as the aging time prolongs, the cyclic peak stress decreases and the plastic strain increases. Khisheh et al. [23] studied the effect of heat treatment on the high cycle bending fatigue performance of an A380 aluminum alloy and the fracture behavior of the material under stress-controlled cyclic loading. The research results showed that heat treatment can improve the high cycle bending fatigue life at the highest and lowest stress levels, and the heat-treated specimens showed a brittle fracture behavior. Liu et al. [24] studied the influence of factors such as over-fire temperature, cooling method and over-fire time on the residual mechanical properties of 6061-T6 aluminum alloy extruded profiles after fire and high temperature treatment through static tensile and repeated hysteretic tests. The research results showed that the strength of the material decreased significantly and the elastic modulus changed little after the fire and high temperature. The over-fire temperature and over-fire time are main factors affecting the strength.

However, there are few studies on the cyclic loading mechanical properties of 6061 aluminum alloy extruded tubes under secondary heat treatment conditions. To further explore the performance characteristics of aluminum alloy after cyclic loading, a 6061-T6 aluminum alloy extruded pipe was taken as the research object, and the effects of different heat treatment process parameters on the cyclic mechanical properties of the alloy were studied by means of a heat treatment test and cyclic tensile test, and the impact of different loading systems on the mechanical properties of the 6061-T6 aluminum alloy without secondary heat treatment was discussed to provide theoretical guidance for the process optimization and industrial production of 6061 aluminum alloys.

## 2. Materials and Methods

The material used in the study is a 6061-T6 aluminum alloy extruded tube with a thickness of 5 mm and an outer diameter of 100 mm produced by Jiangsu Yimai Aluminum Industry Group(Wuxi, China). Its chemical composition are as follows (wt.%): 0.4–0.8 Si, 0.8–1.2 Mg, 0.7 Fe, 0.15–0.4 Cu, 0.15 Mn, 0.04–0.35 Cr, 0.25 Zn, 0.15 Ti and residual Al. Regarding the GB/T 228.1-2010 standard [25], the arc-shaped tensile specimens are taken along the axial direction of the pipe, and the final size parameters of the specimens are shown in Figure 1.

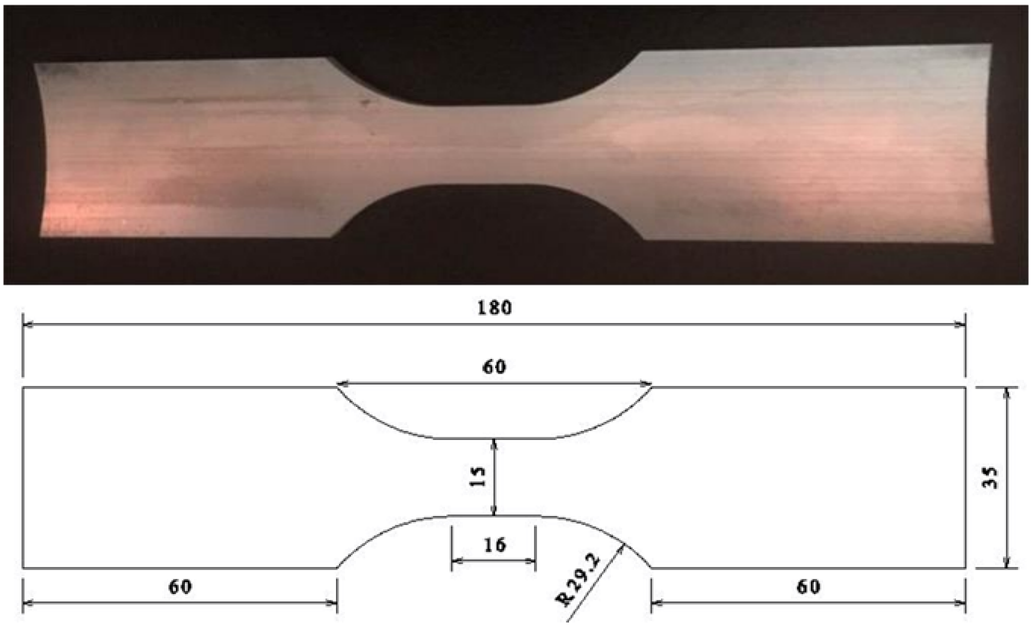


**Figure 1.** Dimension of the 6061 aluminum alloy specimen (dimensions are in mm).

To study the effects of different heat treatment processes on the mechanical properties of 6061 aluminum alloy extruded tubes under cyclic loading, heat treatment tests, and cyclic tensile loading tests were carried out. The heat treatment process scheme, as shown in Table 1, is designed in the way of single-variable control, and the heat treatment test is carried out on the 6061 aluminum alloy. Then, the cyclic tensile tests are carried out on the 6061 aluminum alloy samples after secondary heat treatment and the aluminum alloy samples without heat treatment. The cyclic tensile test device is shown in Figure 2 and the loading control method adopts program-controlled force loading. Ten kinds of loading systems were designed in the test, as shown in Table 2 and Figure 3.

**Table 1.** Heat treatment processes of the 6061 aluminum alloy.

| Number | Heating Temperature | Holding Time | Cooling Method |
|---|---|---|---|
| 1 | 410 °C, 440 °C, 470 °C, 500 °C, 530 °C, 560 °C | 2 h | Air cooling (AC) |
| 2 | 560 °C | 1 h, 2 h, 3 h, 4 h, 5 h | Air cooling (AC) |
| 3 | 560 °C | 4 h | Air cooling (AC), water quenching (WQ), furnace cooling (FC) |

**Table 2.** The loading systems of the 6061 aluminum alloy specimen.

| Number | Loading Pattern |
|---|---|
| Ls1 | Monotonic |
| Ls2 | Under cyclic tensile loading, the loading displacement is 2 mm/min, and the stress amplitude is 6000 N for 10 cycles |
| Ls3 | Under cyclic tensile loading, the loading displacement is 2 mm/min, and the stress amplitude is 9000 N for 10 cycles |
| Ls4 | Cyclic tensile loading, loading displacement of 2 mm/min, loading with a 12,000 N stress amplitude for 10 cycles |

**Table 2.** *Cont.*

| Number | Loading Pattern |
|---|---|
| Ls5 | Cyclic tensile loading, loading displacement of 2 mm/min, with a stress increment of 1000 N, loading to 6000 N, one cycle for each stage and three cycles for the last stage |
| Ls6 | Cyclic tensile loading, loading displacement of 2 mm/min, loading to 6000 N with a stress increment of 1000 N, two cycles per stage and three cycles of the last stage |
| Ls7 | Cyclic tensile loading, loading displacement of 2 mm/min, loading to 6000 N with a stress increment of 1000 N, three cycles per stage and six cycles at the last stage |
| Ls8 | Cyclic tensile loading, loading displacement of 2 mm/min, loading to 9000 N with a stress increment of 1500 N, one cycle for each stage and three cycles for the last stage |
| Ls9 | Cyclic tensile loading, loading displacement of 2 mm/min, loading to 9000 N with a stress increment of 1500 N, two cycles per stage and three cycles of the last stage |
| Ls10 | Cyclic tensile loading, loading displacement of 2 mm/min, loading to 9000 N with a stress increment of 1500 N, three cycles per stage and six cycles at the last stage |

**Figure 2.** Test loading device.

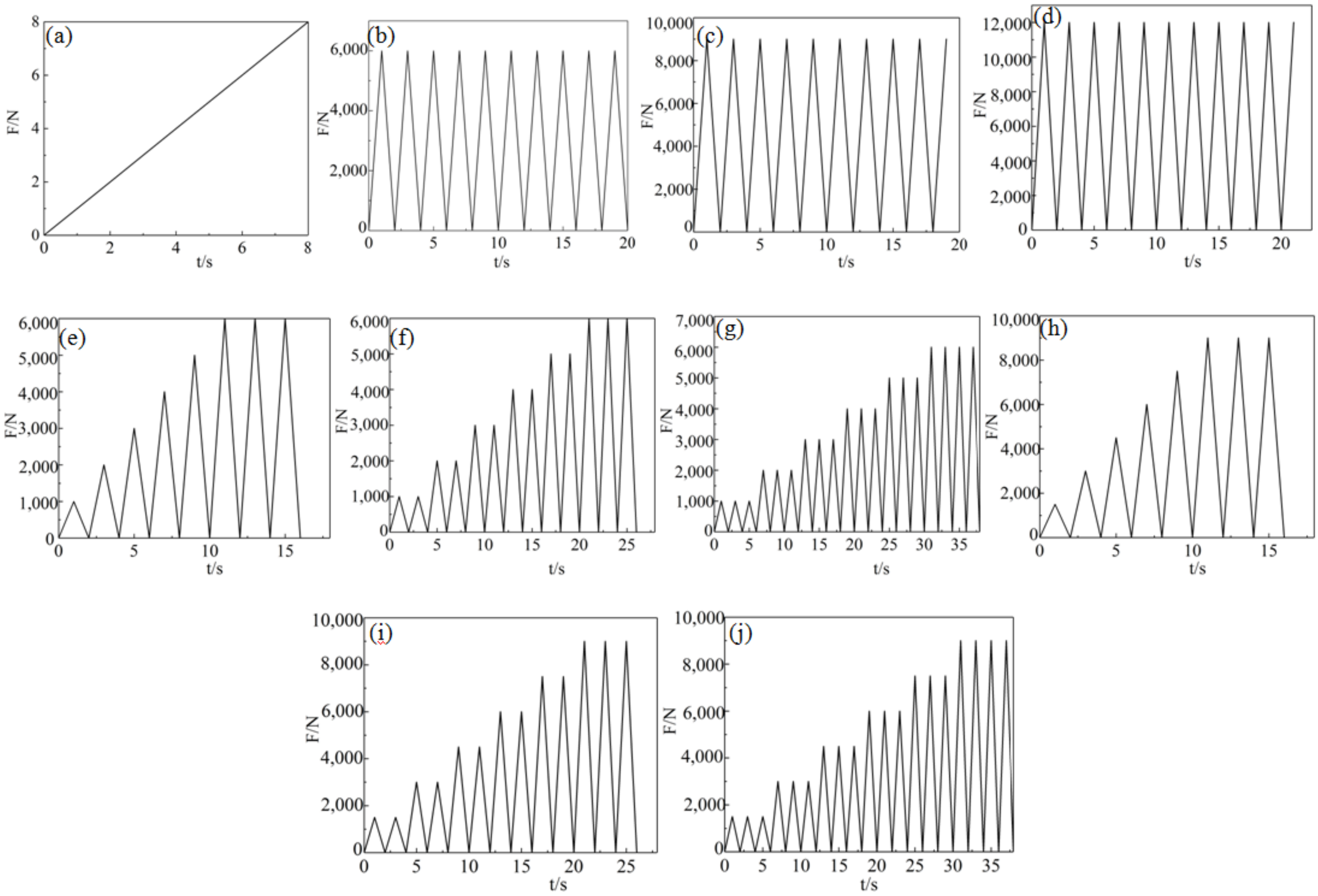

**Figure 3.** Sketches of the loading system: (**a**) Ls1, (**b**) Ls2, (**c**) Ls3, (**d**) Ls4, (**e**) Ls 5, (**f**) Ls6, (**g**) Ls7, (**h**) Ls8, (**i**) Ls9, (**j**) Ls10.

## 3. Experiment Results and Analysis

The results of monotonic and cyclic tensile tests of the specimen are shown in Tables 3 and 4, where $f_{0.2}$ is the tensile strength (yield strength) when the residual strain is 0.2%, $f_{u1}$ is the ultimate tensile strength, $f_{u2}$ is the fracture stress, $\varepsilon_1$, $\varepsilon_{u1}$ and $\varepsilon_{u2}$ are the strain corresponding to yield strength, ultimate tensile strength and fracture stress, respectively, $A$ is the elongation, $N$ is the number of loops of hysteresis and $E$ is the hysteresis energy.

**Table 3.** Test results of the 6061 aluminum alloy after secondary heat treatment.

| Specimens | Loading System | $f_{0.2}$ (MPa) | $f_{u1}$ (MPa) | $f_{u2}$ (MPa) | $\varepsilon_1$ (%) | $\varepsilon_{u1}$ (%) | $\varepsilon_{u2}$ (%) | $A$/% | $N$ | $E$ (KN·mm) |
|---|---|---|---|---|---|---|---|---|---|---|
| 25 °C | Ls5 | 62.6 | 352.57 | 275.9 | 0.0214 | 0.464 | 0.499 | 25 | 8 | 7.196 |
| 410 °C | Ls5 | 42.08 | 149.11 | 117.34 | 0.02 | 0.438 | 0.524 | 50 | 8 | 12.39 |
| 440 °C | Ls5 | 46.82 | 197.001 | 148.902 | 0.02 | 0.546 | 0.625 | 46.25 | 8 | 21.85 |
| 470 °C | Ls5 | 65.7 | 269.64 | 201.01 | 0.02 | 0.606 | 0.669 | 54.53 | 8 | 6.099 |
| 500 °C | Ls5 | 56.53 | 240.96 | 173.91 | 0.024 | 0.6835 | 0.727 | 43.75 | 8 | 27.34 |
| 530 °C | Ls5 | 54.68 | 275.74 | 193.31 | 0.0207 | 0.743 | 0.813 | 66.87 | 8 | 23.37 |
| 560 °C | Ls5 | 55.96 | 266.48 | 190.4 | 0.02 | 0.71 | 0.743 | 58.12 | 8 | 12.74 |
| 1 h | Ls5 | 53.05 | 269.43 | 190.5 | 0.022 | 0.732 | 0.779 | 66.87 | 8 | 26.35 |
| 3 h | Ls5 | 50.81 | 321.45 | 211.32 | 0.022 | 0.898 | 0.935 | 78.87 | 8 | 37.92 |
| 4 h | Ls5 | 51.06 | 243.45 | 175.12 | 0.022 | 0.686 | 0.734 | 60.62 | 8 | 25.1 |
| 5 h | Ls5 | 45.13 | 251.32 | 177.84 | 0.02 | 0.73 | 0.771 | 61.9 | 8 | 32.59 |

**Table 4.** Test results of the 6061 aluminum alloy without secondary heat treatment.

| Specimen | Loading System | $f_{0.2}$ (MPa) | $f_{u1}$ (MPa) | $f_{u2}$ (MPa) | $\varepsilon_1$ (%) | $\varepsilon_{u1}$ (%) | $\varepsilon_{u2}$ (%) | *A*/% | *N* | *E* (KN·mm) |
|---|---|---|---|---|---|---|---|---|---|---|
| 1 | Ls1 | 150.5 | 309.55 | 275.89 | 0.0363 | 0.328 | 0.361 | 31.25 | Monotonic | 102.56 |
| 2 | Ls2 | 69.82 | 337.91 | 270.97 | 0.0207 | 0.389 | 0.428 | 21.25 | 10 | 5.6 |
| 3 | Ls3 | 69.82 | 341.38 | 272.102 | 0.0201 | 0.395 | 0.433 | 31.25 | 10 | 33.66 |
| 4 | Ls4 | 69.92 | 357.1 | 280.43 | 0.021 | 0.445 | 0.49 | 21.87 | 10 | 82.74 |
| 5 | Ls5 | 62.6 | 352.57 | 275.9 | 0.0214 | 0.464 | 0.499 | 25 | 8 | 7.196 |
| 6 | Ls6 | 72 | 336.82 | 261.46 | 0.0206 | 0.392 | 0.42 | 31.25 | 13 | 2.643 |
| 7 | Ls7 | 64.4 | 337.13 | 288.81 | 0.0203 | 0.533 | 0.571 | 37.5 | 21 | 8.869 |
| 8 | Ls8 | 68.65 | 349.97 | 279.27 | 0.02 | 0.426 | 0.447 | 31.25 | 8 | 16.52 |
| 9 | Ls9 | 66.85 | 359.7 | 272.72 | 0.02 | 0.447 | 0.463 | 25 | 13 | 20.254 |
| 10 | Ls10 | 62.6 | 355.17 | 279.19 | 0.0156 | 0.431 | 0.463 | 31.25 | 21 | 22.018 |

To analyze the effect of heat treatment process parameters on the cyclic tensile loading properties of the 6061 aluminum alloy, the cyclic stress–strain curves of the alloy under different heating temperatures, holding times and cooling methods were obtained through cyclic tensile loading tests under the same loading system. Through comparative analysis, the influence of different heat treatment process parameters on the cyclic loading results of the 6061 aluminum alloy was determined.

### 3.1. Effect of Heating Temperature on Cyclic Stress–Strain Curves

According to the loading system Ls5 shown in Table 3, the 6061 aluminum alloy samples under different heating temperatures of 410 °C, 440 °C, 470 °C, 500 °C, 530 °C and 560 °C were subjected to cyclic tensile tests, and the cyclic stress–strain curves of the alloy under different heating temperatures were obtained, as shown in Figure 4.

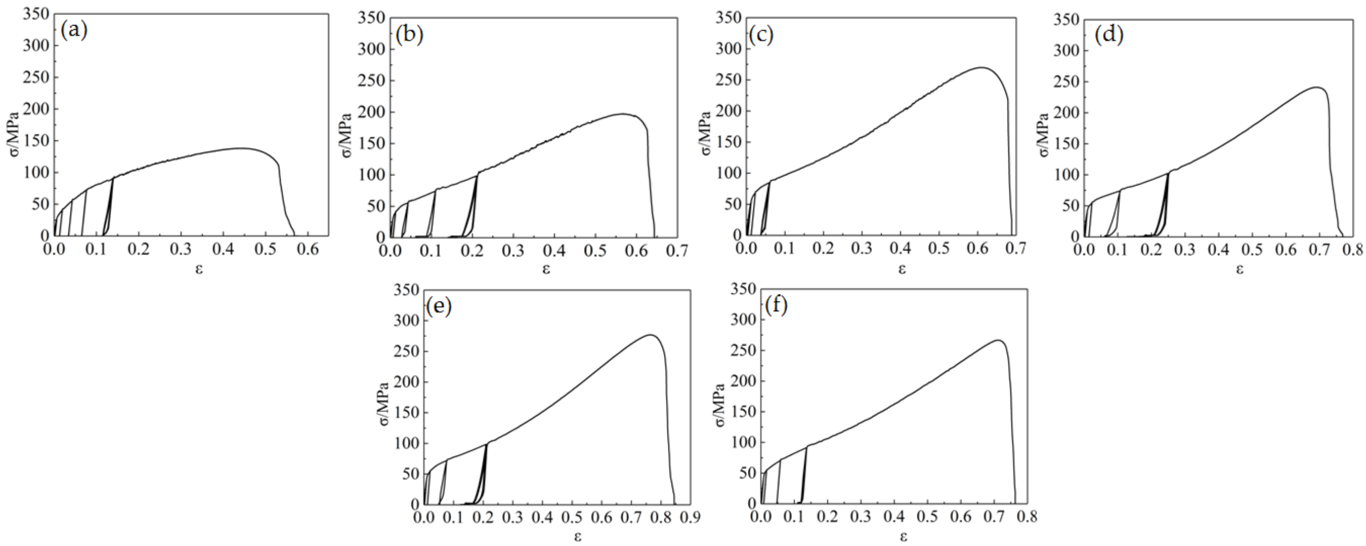


**Figure 4.** Stress–strain curves of the 6061 aluminum alloy under different heat treatment temperatures of (**a**) 410 °C, (**b**) 440 °C, (**c**) 470 °C, (**d**) 500 °C, (**e**) 530 °C, (**f**) 560 °C.

According to the cyclic stress–strain curves of the 6061 aluminum alloy at different heating temperatures shown in Figure 4, under low-stress-controlled cyclic loading, the loading and unloading curves of the alloy coincide. With the increase in the number of cycles, the hysteresis loop structure tends to be stable. With the increase in the cyclic stress level, there are obvious differences in the hysteresis loop shape of the alloy at different heating temperatures. When the heating temperature increases from 410 °C to 560 °C, the plastic strain in the cyclic hysteresis curve of the alloy shows a bimodal change with the increased heating temperature. It can be seen that the 6061 aluminum alloy after secondary heat treatment exhibits obvious hysteresis behavior during multi-level stress-controlled cyclic tensile loading at different heating temperatures.

The yield strength, tensile strength and uniform elongation curve of the 6061 aluminum alloy with heating temperature are shown in Figure 5 according to the test results in Table 3.

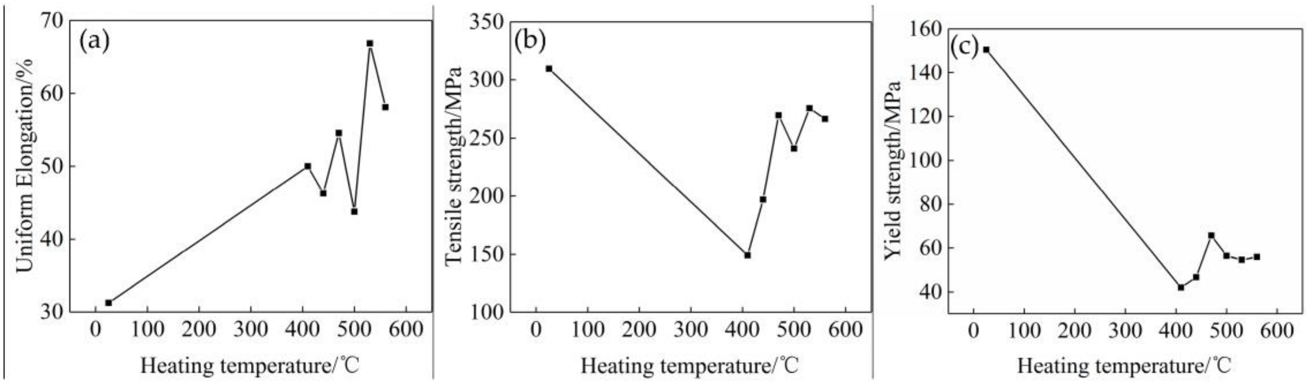


**Figure 5.** Variation curves of uniform elongation (**a**), tensile strength (**b**) and yield strength (**c**) with heating temperature.

According to the variation curves of the yield strength, tensile strength and uniform elongation with heating temperature shown in Figure 5, it can be seen that as the heating temperature increases from 25 °C to 560 °C, the yield strength and tensile strength of the alloy shows a trend of decreasing first, then increasing and then decreasing, while the uniform elongation fluctuates with the increase in heating temperature.

### 3.2. Effect of Holding Time on Cyclic Stress–Strain Curves

After analyzing the effects of heating temperature on the cyclic loading properties of the 6061 aluminum alloy, the effects of different holding time on the cyclic loading properties are studied through cyclic tensile tests, and the cyclic loading stress–strain curves of the 6061 aluminum alloy under different holding time conditions are obtained, as shown in Figure 6.

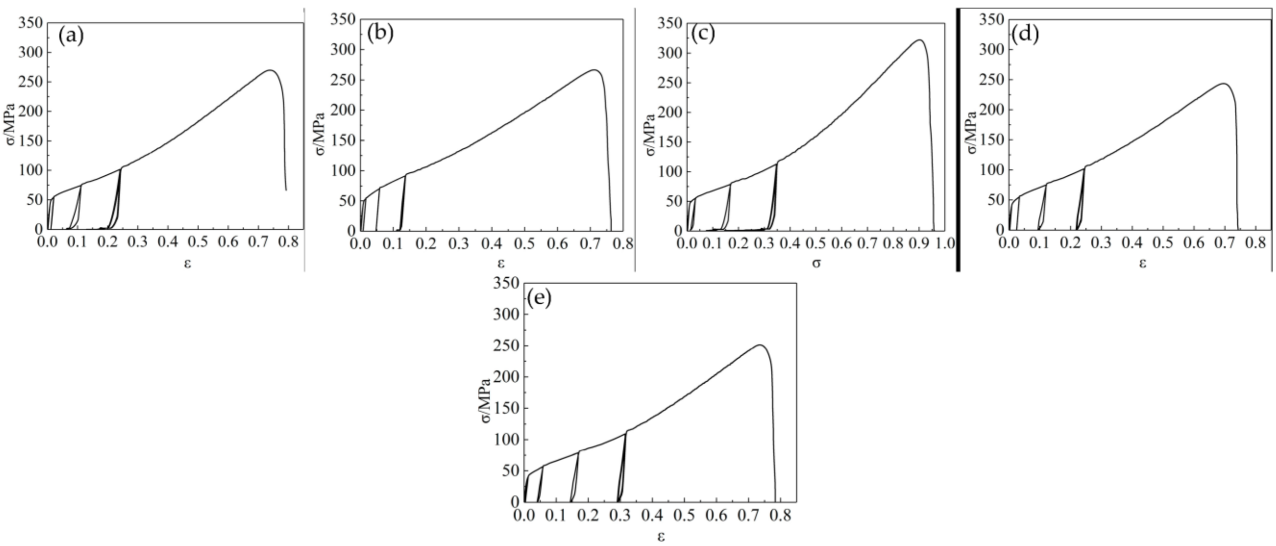


**Figure 6.** Stress–strain curves of the 6061 aluminum alloy under different holding times: (**a**) 1 h, (**b**) 2 h, (**c**) 3 h, (**d**) 4 h, (**e**) 5 h.

According to the cyclic stress–strain curves of the 6061 aluminum alloy under different holding times, shown in Figure 6, it can be seen that under low-stress-controlled cyclic loading, the loading and unloading curves of the alloy coincide. With the increase in the number of cycles, the hysteresis loop structure tends to be stable. With the increase in the cyclic stress lever, there are certain differences in the shape of the hysteresis loop of the alloy at different holding times. When the holding time is extended from 1 h to 5 h, the response of plastic strain fluctuates with the prolongation of the holding time. It can be seen that the alloy after secondary heat treatment has obvious hysteresis behavior under multi-stage stress-controlled cyclic tensile loading under different holding times, and the response of plastic strain increases with the increase in the stress amplitude.

According to the test results in Table 3, the variation curves of yield strength, tensile strength and uniform elongation of the 6061 aluminum alloy is plotted against holding time, as shown in Figure 7.

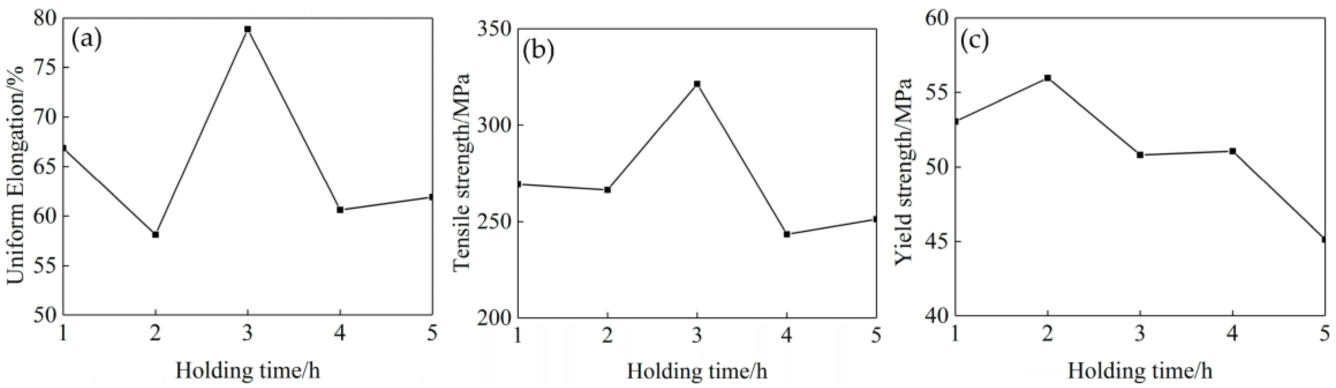


**Figure 7.** Variation curves of uniform elongation (**a**), tensile strength (**b**) and yield strength, (**c**) against holding time.

According to the curve shown in Figure 7, it can be seen that the tensile strength and uniform elongation of the 6061 aluminum alloy show a trend of first decreasing, then increasing and then decreasing when the holding time is extended from 1 h to 5 h, both reaching their maximum values at a holding time of 3 h. On the other hand, the yield strength shows a fluctuating trend with the extension of insulation time.

### *3.3. Effect of Cooling Method on Cyclic Stress–Strain Curves*

After analyzing the influence of heating temperature and holding time on the cyclic loading performance of the 6061 aluminum alloy, the influence of different cooling methods on the cyclic loading performance of the alloy is studied using a universal tensile testing machine, and the cyclic loading stress–strain curves of the alloy under different cooling methods are obtained, as shown in Figure 8.

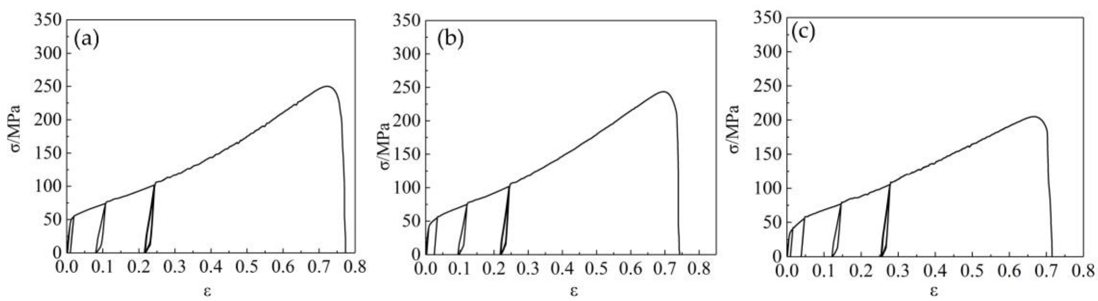


**Figure 8.** Stress–strain curves of the 6061 aluminum alloy under different cooling methods: (**a**) WQ, (**b**) AC, (**c**) FC.

According to the cyclic stress–strain curves of the 6061 aluminum alloy under different cooling methods shown in Figure 8, it can be seen that under low-stress-controlled cyclic loading, the loading and unloading curves of the alloy under different cooling methods coincide. With the increase in the number of cycles, the hysteresis loop structure tends to be stable. With the increase in the cyclic stress level, there is little difference in the shape of hysteresis loops of the alloy under different cooling modes. The width of the hysteresis curve of the alloy under air cooling and water quenching is similar, but the width of the hysteresis curve of the alloy under furnace cooling is relatively large. It can be seen that different cooling methods have little effect on the hysteretic properties of the alloy. According to the tensile curve after cyclic loading, the plastic performance of the 6061 aluminum alloy under water quenching is better than that under air cooling and furnace cooling, with furnace cooling having the worst plastic performance.

According to the test results in Table 3, the variation curves of yield strength, tensile strength and uniform elongation of the 6061 aluminum alloy is plotted against cooling method, as shown in Figure 9.

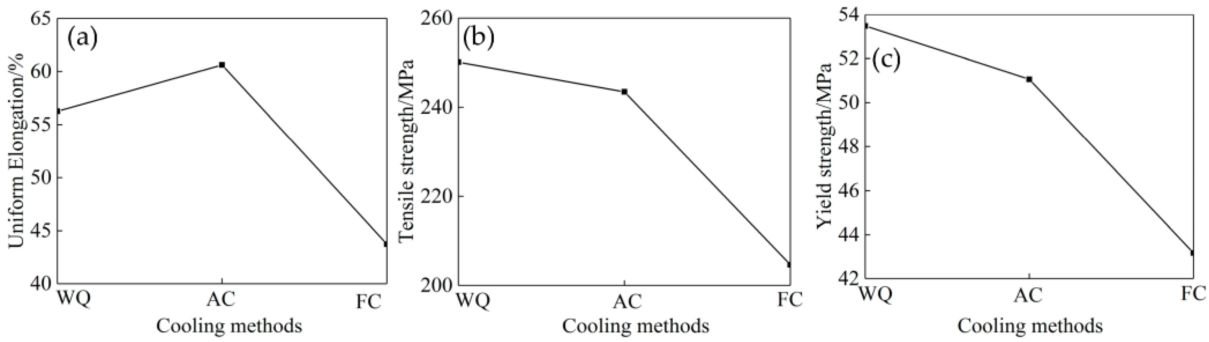


**Figure 9.** Variation curves of uniform elongation (**a**), tensile strength (**b**) and yield strength, (**c**) against cooling method.

According to the curves in Figure 9, it can be seen that the three different cooling methods of water quenching, air cooling and furnace cooling have a significant impact on the ultimate tensile strength of 6061 aluminum alloy specimens after loading. Under water quenching, the yield strength and ultimate tensile strength of the alloy are slightly higher than those under air cooling, while its uniform elongation is slightly lower than that under air cooling. The yield strength, ultimate tensile strength and uniform elongation under furnace cooling are lower than those under water quenching and air cooling.

Comparing the data in Figures 5, 7 and 9, it can be seen that the yield strength, tensile strength and uniform elongation of aluminum alloys under different heat treatment conditions are dispersed. This also reflects that the heating temperature of heat treatment has a significant impact on the mechanical properties of the alloy, followed by the insulation time, and the cooling method has the smallest impact on the mechanical properties of the alloy.

### *3.4. Effects of Different Loading Systems on Cyclic Stress–Strain Curves*

The stress–strain curve of the 6061 aluminum alloy tube without secondary heat treatment was obtained using the monotonic loading test, as shown in Figure 10. The stress–strain curve of the alloy tube increases with the increase in the strain, and there is no obvious yield platform on the stress–strain curve; its yield strength and the ultimate strength are 150.5 Mpa and 309.55 Mpa, respectively.

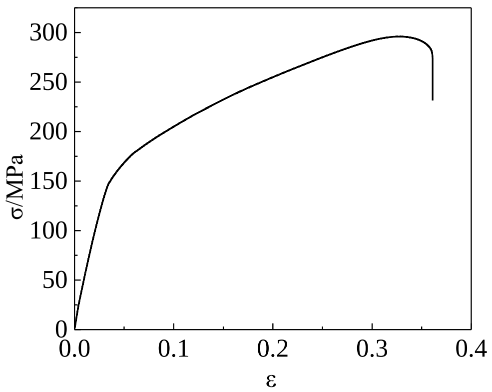


**Figure 10.** Stress–strain curve of the 6061 aluminum alloy without secondary heat treatment.

After obtaining the monotonic tensile properties of the 6061 aluminum alloy without secondary heat treatment, cyclic tensile loading tests on the alloy are continued through a universal tensile testing machine, and the cyclic stress–strain curves under different cyclic loading systems are obtained, as shown in Figure 11.

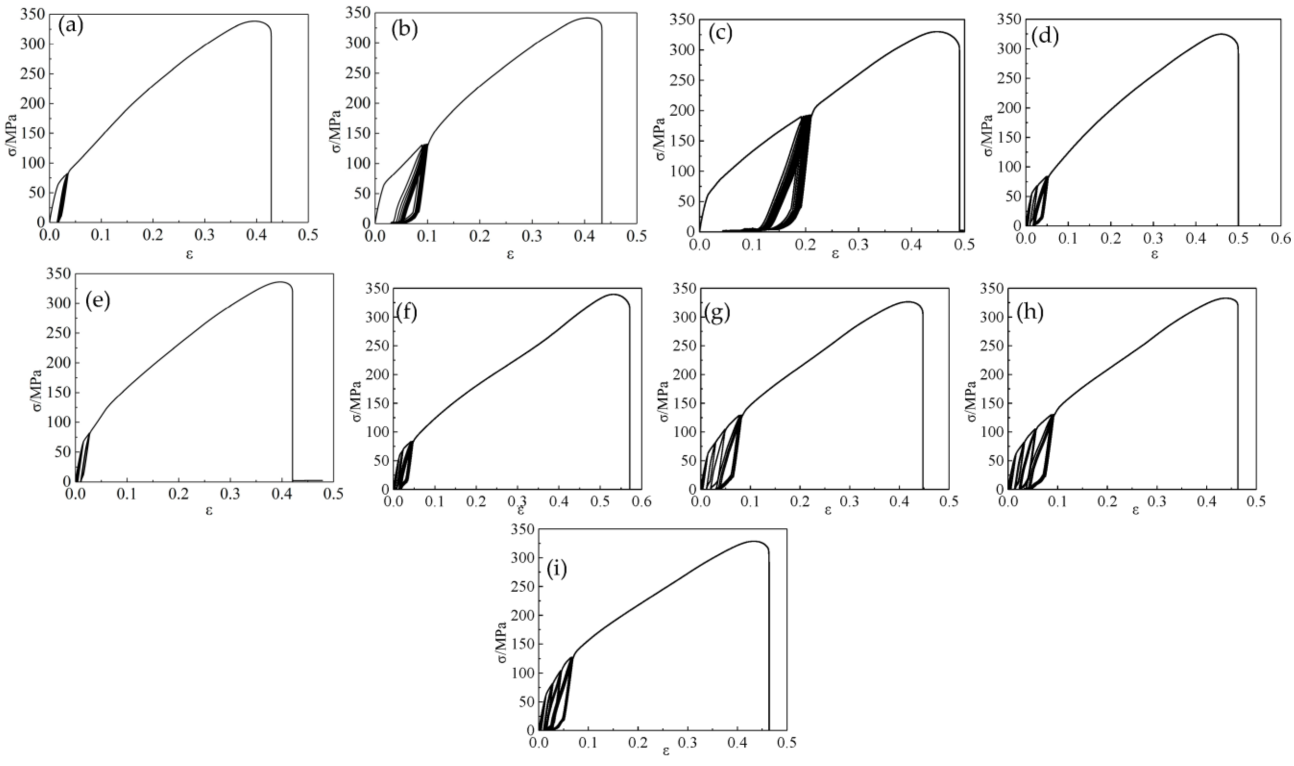


**Figure 11.** Cyclic stress–strain curves of the 6061 aluminum alloy without secondary heat treatment: (**a**) 2, (**b**) 3, (**c**) 4, (**d**) 5, (**e**)6, (**f**) 7, (**g**) 8, (**h**) 9, (**i**) 10.

According to the cyclic loading stress–strain curves of the 6061 aluminum alloy without secondary heat treatment under different loading regimes shown in Figure 11, it can be seen that the hysteretic behavior of the specimens depends on the applied stress level and the number of cycles during the stress-controlled cyclic loading process. Compared with Figure 11a–c, as the stress amplitude increases from 6000 N to 12,000 N, the hysteresis curve of the alloy gradually broadens and the response of plastic strain and hysteretic energy increase gradually, indicating that there is plastic dissipation during each cyclic loading process. After a certain number of cycles, the stress hysteresis curve of the alloy remains unchanged. Compared with Figure 11d,e, it can be seen that the multi-loop hysteresis will lead to an early fracture of the alloy material. Compared with Figure 11d,g,

Figure 11e,h, Figure 11f and Figure 11i, it can be seen that during the multi-stage stress cycling loading process, the hysteretic behavior of the specimen depends not only on the current stress level, but also on the previous loading history. The hysteresis behavior at the previous smaller stress amplitude has little effect on the hysteresis behavior at the subsequent larger stress amplitude. As the tensile stress continues to increase, the width of the hysteresis curve and the plastic strain value after unloading also increase gradually. The stress–strain curves of the specimen under multi-stage cyclic loading all show obvious nonlinear characteristics, mainly due to the continuous decrease in its elastic modulus and the continuous accumulation of plastic strain.

Compared with Figures 4, 6, 8, 10 and 11, it can be seen that there is no obvious yield platform for the 6061 aluminum alloy under monotonic and cyclic loading. During the elastic deformation stage, the cyclic loading and unloading stress–strain curves of the alloy coincided, which is mainly because the plastic deformation caused by the load is very small, and the damage degree of the alloy material is low. With the increase in cyclic stress level, the alloy enters the yield stage, the internal damage of the material develops rapidly, and the inelastic deformation caused by loading and unloading gradually increases.

Based on the test results in Table 4, the variation curves of yield strength, tensile strength and uniform elongation of the 6061 aluminum alloy are plotted against different loading regimes, as shown in Figure 12.

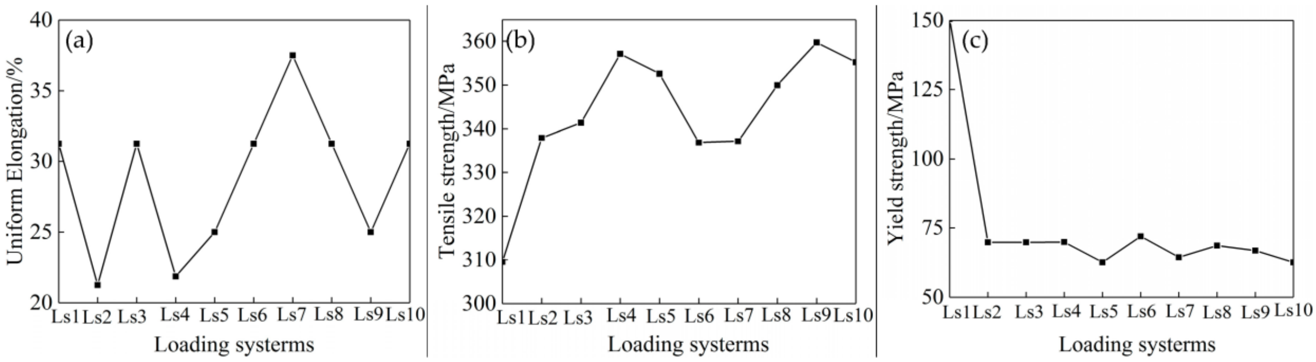


**Figure 12.** Variation curves of uniform elongation (**a**), tensile strength (**b**) and yield strength (**c**) against loading systems.

According to the curves in Figure 12, it can be seen that different loading systems have a significant impact on the yield strength, tensile strength and uniform elongation of the 6061 aluminum alloy. The yield strength of the alloy under loading system Ls1 is significantly higher than that under other loading systems. On the other hand, their ultimate tensile strength is significantly lower than that under other loading systems and the uniform elongation of the alloy fluctuates under different loading systems.

### 3.5. Hysteretic Energy

The work absorbed or the energy consumed when a metal material undergoes plastic deformation is the hysteresis energy. The width and size of the hysteresis curve reflect the ability of a material to resist plastic deformation. In the cyclic deformation of materials, the magnitude of hysteresis energy is equal to the area enclosed by its corresponding hysteresis curve. The origin lab software is used to calculate the hysteresis energy corresponding to the hysteresis curve of the 6061 aluminum alloy under different cyclic tensile loading, and the hysteresis energy histogram of the 6061 aluminum alloy specimen drawn under different loading regimes, as shown in Figure 13.

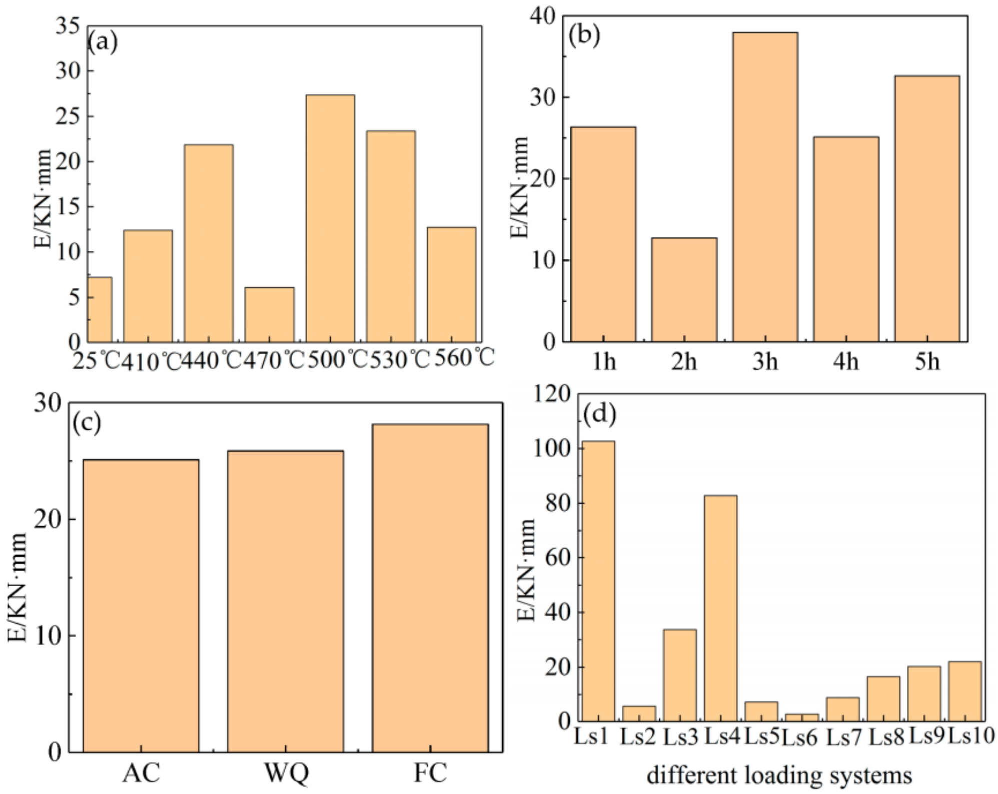


**Figure 13.** Energy dissipation of the 6061 aluminum alloy (**a**) under Ls5 with different heating temperatures, (**b**) under Ls5 with different holding times, (**c**) under Ls5 with different cooling methods, (**d**) under different loading systems.

According to the hysteresis energy of the 6061 alloy specimen under different loading regimes, shown in Figure 13, it can be seen that different heat treatment process parameters and cyclic loading regimes have certain effects on the hysteresis energy. According to the hysteretic energy histogram of the alloy in Figure 13a–c, it can be seen that under the same loading system, the heating temperature, holding time and cooling method of heat treatment have a certain impact on the hysteresis energy of the alloy. With the heating temperature increasing from 25 °C to 560 °C, the hysteresis energy of the specimen after the second heating treatment shows a bimodal trend. When the heating temperature is 470 °C, the hysteresis energy of the alloy is the smallest, slightly lower than that of the 6061 aluminum alloy without secondary heat treatment. With the extension of holding time from 1 h to 5 h, the hysteresis energy of the specimen after heat treatment showed a fluctuating trend. The hysteresis energy of the alloy is not much different under three different cooling methods, i.e., air cooling, water quenching and furnace cooling.

Comparing the cyclic loading regimes Ls2, Ls3 and Ls4 in Figure 13d, it can be seen that the hysteretic energy of the specimen without secondary heat treatment increases with the increase in stress amplitude, which indicates that the alloy consumes a large amount of energy under cyclic loading. Comparing the loading systems Ls5, Ls6, Ls7, Ls8, Ls9 and Ls10 in Figure 13b, it can be seen that under the same number of cycles, the hysteresis energy of the alloy specimens under loading regimes Ls5, Ls6 and Ls7 is significantly lower than that under loading regimes Ls8, Ls9 and Ls10. This indicates that the cyclic loading regime and the applied stress level have a certain impact on the hysteresis energy. The hysteretic energy of the specimens without secondary heat treatment increases with the increase in the number of cycles, indicating that the aluminum alloy exhibits good energy dissipation ability under cyclic loading. Comparing the loading regimes Ls5, Ls6 and Ls7 in Figure 13b, it can be seen that as the number of cycles increases, the hysteresis energy of the alloy first decreases and then increases. Comparing the loading regimes Ls8, Ls9 and

Ls10, it can be seen that as the number of cycles increases, the hysteresis energy of the alloy increases gradually, which indicates that the relationship between the number of cycles and hysteresis energy is not monotonous. Further, sample 6 has experienced 13 cycles of cyclic loading, while the sample 10 has experienced 21 cycles of cyclic loading. The hysteretic energy of sample 6 is significantly lower than that of sample 10. The hysteresis energy of sample 6 decreases and the ductility deteriorates. The main reason is that after the test piece has undergone multi-stage cyclic loading, the cumulative effect of plastic damage is obvious, which leads to the continuous development of internal cracks and early failure of the specimen.

From the above analysis, it can be concluded that different heat treatment process parameters, applied stress levels, cyclic loading times and loading systems have a certain impact on the hysteresis energy of the aluminum alloy, and the relationship between cyclic loading times and hysteresis energy is not monotonous.

### 3.6. Skeleton Curve

The cyclic skeleton curve is a curve obtained by translating and connecting the sections of the cyclic loading stress–strain curve that exceed the maximum stress of the previous loading, which is called the skeleton curve. Figure 14 shows the skeleton curves of 6061 aluminum alloy specimens under different cyclic loading regimes.

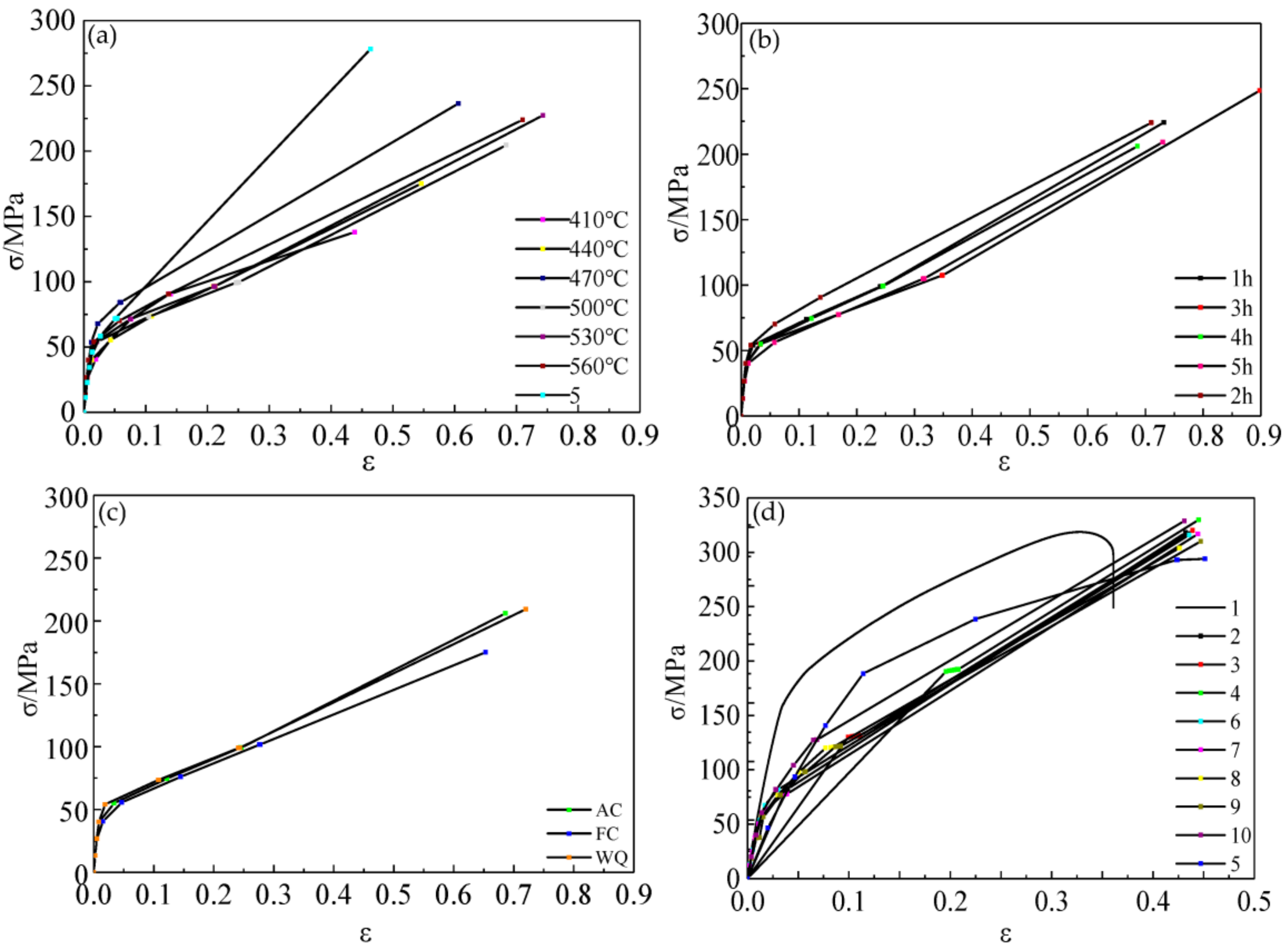


**Figure 14.** Skeleton curves of the 6061 aluminum alloy (**a**) under Ls5 with different heating temperatures, (**b**) under Ls5 with different holding times, (**c**) under Ls5 with different cooling methods and (**d**) under different loading patterns.

According to the monotonic and cyclic loading skeleton curves of 6061 aluminum alloy specimens shown in Figure 14, it can be seen that different heat treatment process parameters and cyclic loading systems have a significant impact on the yield strength and ultimate tensile strength of the alloy. Compared with the curves in Figure 14a, the strength of the specimen increases with the heating temperature from 25 °C to 560 °C, it shows a sharp decrease first and then a gradual increase, while the uniform elongation fluctuates. Compared with the curves in Figure 14b, different heat treatment holding times have little effect on the yield strength of the alloy, but have a greater effect on the ultimate tensile strength and elongation. Compared with the curves in Figure 14c, the yield strength, tensile strength and elongation of the alloy under furnace cooling are lower than those under air cooling and water quenching. The three different cooling methods of air cooling, water quenching and furnace cooling have a great impact on the ultimate tensile strength of the alloy specimens in the later stage of loading, and the effects of air cooling and water quenching on the yield strength and uniform elongation of the alloy during cyclic stretching are relatively small.

Comparing the curves in Figure 14d, it can be seen that the cyclic tensile skeleton curve of the 6061 aluminum alloy without secondary heat treatment does not coincide with the monotonic tensile test curve, and the cyclic loading stress–strain curve enters the yield zone ahead of time, while the elastic section of the monotonic tensile stress–strain curve is longer. Different cyclic loading systems have a significant impact on the ultimate tensile strength and elongation of the alloy specimens in the later stage of loading.

Based on the above analysis, it can be concluded that the heating temperature of reheat treatment has a great impact on the cyclic loading performance of 6061 aluminum alloy extruded tubes, followed by the insulation time. The cooling method has a relatively small impact on the cyclic loading performance of alloy extruded tubes.

### 3.7. Test Phenomenon

During the test, the 6061 aluminum alloy specimens after secondary heat treatment have obvious deformation and necking before the damage, as shown in Figure 15. The specimens without secondary heat treatment show no necking phenomenon during the process of breaking after cyclic loading, and the failure is accompanied by a loud noise and the fracture morphology is shown in Figure 16. The damaged fracture of the specimen without secondary heat treatment is relatively flat, with no obvious deformation and cross-section shrinkage at the edge, and no obvious necking section. According to Tables 3 and 4, the elongation of the specimen without secondary heat treatment is lower than that of the specimen after secondary heat treatment, which indicates that the plasticity of the specimen without secondary heat treatment is weaker than that of the specimen after secondary heat treatment.

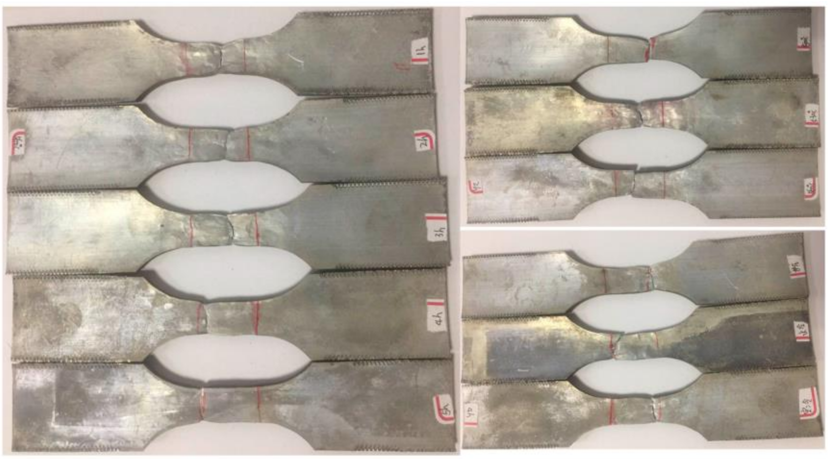

**Figure 15.** Fracture diagrams of the 6061 aluminum alloy specimen after secondary heat treatment.

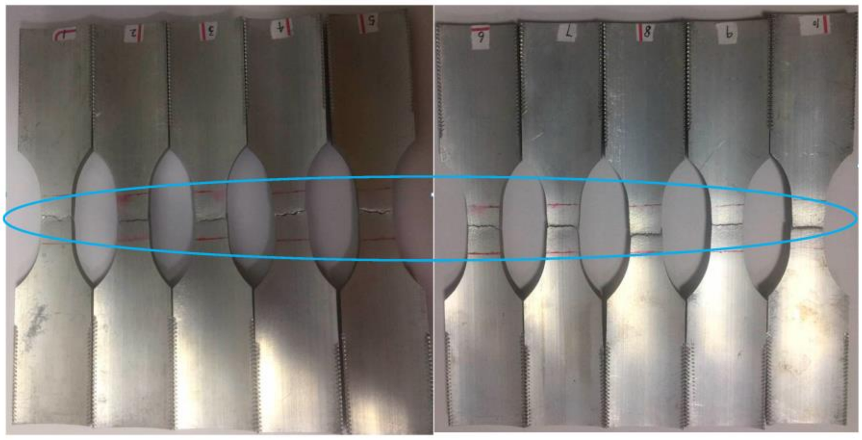

**Figure 16.** Tensile fracture diagrams of the 6061 aluminum alloy specimen without secondary heat treatment. The blue line marks the location of the fracture.

## 4. Conclusions

(1) Under the selected test conditions, compared with the effects of insulation time and cooling method during heat treatment on the cyclic tensile comprehensive strength performance of the 6061 aluminum alloy, the heating temperature plays a primary role, the cooling method plays a secondary role and the holding time plays a minimal role.

(2) The cyclic stress–strain curve of the 6061 aluminum alloy depends on the applied stress level and loading history. At low stress levels, the loading and unloading curves in the cyclic stress–strain curve of the specimen coincide. With the increase in tensile stress, the hysteresis energy of the specimen gradually increases. As the number of cycles increases, the shape of the hysteresis loop of the specimen tends to stabilize, but there is no monotonic relationship between the number of cycles loaded and the hysteresis energy.

(3) The cyclic loading system has a significant impact on the yield strength, tensile strength, elongation and hysteresis energy of the 6061 aluminum alloy. Under the monotonic loading system, the ultimate tensile strength and uniform elongation of the alloy were 309.55 MPa and 31.25%, respectively, which is significantly lower than those of the alloys under other loading systems. Further, its yield strength is significantly lower than those under other loading systems, while the yield strength was 150.5 MPa, which is significantly higher than those of the alloys under other loading systems.

(4) The cyclic tensile skeleton curve of the 6061-T6 aluminum alloy does not coincide with the monotonic loading curve. The cyclic loading stress–strain curve enters the yield section ahead of time, while the elastic section of the monotonic loading stress–strain curve is longer.

(5) The 6061 aluminum alloy specimen, after secondary heat treatment, undergoes significant deformation and necking before the damage, with good plasticity. However, the untreated specimen undergoes cyclic loading and tensile fracture, its fracture surface is relatively flat, with no obvious deformation or cross-section shrinkage at the edges, and the necking section is not obvious. In future research, we will investigate the fracture zoon and microstructure analysis of the cyclic tensile specimens.

**Author Contributions:** Conceptualization, F.D. and T.H.; methodology, T.H., H.Z. and Q.Z.; formal analysis, J.W.; investigation, F.C.; resources, Q.Z.; data curation, T.H.; writing—original draft preparation, T.H.; writing—review and editing, F.D.; visualization, H.Z.; supervision, F.C.; project administration, Q.Z.; funding acquisition, F.D. All authors have read and agreed to the published version of the manuscript.

**Funding:** This research was funded by the Talent introduction project of Anhui University of science and technology (no. RCYJ202105); 2021 School-level Quality Engineering Project of Anhui Science and Technology University (no. X2021081); University Collaborative Innovation Project of Anhui Province: Research and development and application of new self-propelled straw baler (no. GXXT-2019-021); major projects of Natural Science Research in Colleges and Universities in the Anhui Province: Research and development of equipment and system for intelligent picking of eggplant and fruit vegetables and fruits (no. KJ2021ZD0110); Design and Key Technology Research of TFT Silicon Ultrafine Powder Automatic Complete Equipment (no. 880839); Design and Key Technology Research of Multi-Parameter Intelligent Control Instrument Junction Box (no. tzy202218); Traditional Professional Transformation and Upgrading (no. Xj2021015); First-Class Textbook Construction Project (new edition) (Xj2021062); Implementation Strategies and Safeguard Measures for Strengthening Course Process Assessment From the Perspective of Professional Certification (no. X2021017); A small portable floor tile handling and paving trolley (S202210879214); Mountain Survey Robot Based on Biomimetic Earthworm (S202210879222); The Reform and Practice of Cultivation of Industrial and Agricultural Compound Applied Mechanical Talents with "dual integration, three education in one, and four links" (no. X2021110); and Reform and Practice of "One Type and Six Modernizations" Practical Teaching System (X2021113). "The APC was funded by the Talent introduction project of Anhui University of Science and Technology (no. RCYJ202105)".

**Data Availability Statement:** All data, models and codes generated or used during the study appear in the submitted article.

**Conflicts of Interest:** The authors declare no conflict of interest.

## References

1. Jiang, B. *Research on Heat Treatment and Granule Medium Forming Technology of Aa6061 Tube*; Yanshan University: Qinhuangdao, China, 2016. (In Chinese)
2. Wang, Y.; Wang, Z.; Hu, X. Experimental investigation on constitutive relationship of high strength aluminum alloy under cyclic loading. *China Civ. Eng. J.* **2016**, *49*, 1–7. (In Chinese) [CrossRef]
3. Sun, Z. *The Study on Cycle Mechanical Behavior and Microstructure of Ultrafine Crystal 6061 Aluminum Alloy*; Guangxi University: Nanning, China, 2018. (In Chinese)
4. Xiang, P.; Jia, L.J.; Shi, M.; Wu, M. Ultra-low cycle fatigue life of aluminum alloy and its prediction using monotonic tension test results. *Eng. Fract. Mech.* **2017**, *186*, 449–465. [CrossRef]
5. Chi, P.; Xiong, W.; Mu, X.; Zhu, B.; Zhou, J.; Bi, X. Experimental test and simulation calculation of fatigue properties of aluminum–titanium-steel explosive welded connector under tension-compression cyclic loading. *J. Mater. Res. Technol.* **2023**, *24*, 4678–4684. [CrossRef]
6. Kashyzadeh, K.R.; Ghorbani, S. New neural network-based algorithm for predicting fatigue life of aluminum alloys in terms of machining parameters. *Eng. Fail. Anal.* **2023**, *146*, 107128. [CrossRef]
7. Azizian-Farsani, E.; Ghodsiyeh, D.; Akbarzadeh, S.; Khonsari, M.M. Theoretical and experimental analysis of relation between entropy and tension-compression fatigue of aluminum 6061-T6. *J. Braz. Soc. Mech. Sci. Eng.* **2020**, *42*, 111. [CrossRef]
8. Macek, W.; Rozumek, D.; Faszynka, S.; Branco, R.; Zhu, S.P.; Nejad, R.M. Fractographic-fractal dimension correlation with crack initiation and fatigue life for notched aluminium alloys under bending load. *Eng. Fail. Anal.* **2023**, *149*, 107285. [CrossRef]
9. Kakavand, E.; Seifi, R.; Abolfathi, M. An investigation on the crack growth in aluminum alloy 7075-T6 under cyclic mechanical and thermal loads. *Theor. Appl. Fract. Mech.* **2022**, *122*, 103585. [CrossRef]
10. Kebir, T.; Harchouche, Z.E.A.; Elmeiche, A.; Benguediab, M. Dissipated Strain Energy of Aluminum Alloy 6061-T6 Induced by Low Cycle Fatigue. *Int. Inf. Eng. Technol. Assoc.* **2019**, *43*, 329–334. [CrossRef]
11. Lim, H.J.; Lee, Y.J.; Sohn, H. Continuous fatigue crack length estimation for aluminum 6061-T6 plates with a notch. *Mech. Syst. Signal Process* **2019**, *120*, 356–364. [CrossRef]
12. Ogawa, T.; Hasunuma, S.; Kato, S.; Suzuki, S.; Nakamura, Y.; Mano, S.; Miyagawa, K. Crack Growth Characteristics of Aluminum Alloys Dominated by the Mechanisms of Fatigue and Stress Corrosion cracking. *Mater. Trans.* **2019**, *60*, 2346–2352. [CrossRef]
13. Rex, A.V.; Paul, S.K.; Singh, A. The influence of equi-biaxial and uniaxial tensile pre-strain on the low cycle fatigue performance of the AA2024-T4 aluminium alloy. *Int. J. Fatigue* **2023**, *173*, 107699. [CrossRef]
14. Myung, N.; Seo, J.; Choi, N.S. Cyclic elastic modulus and low cycle fatigue life of woven-type GERP coated aluminum plates. *Compos. Part B-Eng.* **2019**, *174*, 107004. [CrossRef]
15. Brammer, A.T.; Jordon, J.B.; Allison, P.G.; Barkey, M.E. Strain-Controlled Low-Cycle Fatigue Properties of Extruded 6061-T6 Aluminum Alloy. *J. Mater. Eng. Perform.* **2013**, *22*, 1348–1350. [CrossRef]
16. Srivatsan, T.S.; Al-Hajri, M.; Hotton, B.; Lam, P.C. Effect of Particulate Silicon Carbide on Cyclic Plastic Strain Response and Fracture Behavior of 6061 Aluminum Alloy Metal Matrix Composites. *Appl. Compos. Mater.* **2002**, *9*, 131–153. [CrossRef]

17. Byakov, A.V.; Eremin, A.V.; Shah, R.T.; Burkov, M.V.; Lyubutin, P.S.; Panin, S.V.; Maruschak, P.O.; Menou, A.; Bencheikh, L. Estimating mechanical state of AA2024 specimen under tension with the use of Lamb wave based ultrasonic technique. *Mol. Cryst. Liq. Cryst.* **2017**, *655*, 94–102. [CrossRef]
18. Pisapia, A.; Nastri, E.; Piluso, V.; Formisano, A.; Mazzolani, F.M. Experimental campaign on structural aluminium alloys under monotonic and cyclic loading. *Eng. Struct.* **2023**, *282*, 115836. [CrossRef]
19. Ding, J.; Kang, G.Z.; Liu, Y.J.; Wang, H.L. Uniaxial time-dependent cyclic deformation of 6061-T6 aluminium alloy. *Chin. J. Nonferrous Met.* **2007**, *17*, 1993–1998. (In Chinese)
20. Guo, X.; Wang, L.; Shen, Z.; Zou, J.; Liu, L. Constitutive model of structural aluminum alloy under cyclic loading. *Constr. Build. Mater.* **2018**, *180*, 643–654. [CrossRef]
21. Zhao, X.; Li, H.; Chen, T.; Cao, B.A.; Li, X. Mechanical Properties of Aluminum Alloys under Low-Cycle Fatigue Loading. *Materials* **2019**, *12*, 2064. [CrossRef]
22. Liu, K.; Mirza, F.A.; Chen, X.G. Effect of Overaging on the Cyclic Deformation Behavior of an AA6061 Aluminum Alloy. *Metals* **2018**, *8*, 528. [CrossRef]
23. Khisheh, S.; Khalili, K.; Azadi, M.; Hendouabadi, V.Z. Influences of roughness and heat treatment on high-cycle bending fatigue properties of A380 aluminum alloy under stress-controlled cyclic loading. *Mater. Chem. Phys.* **2021**, *264*, 124475. [CrossRef]
24. Liu, H.B.; Zhou, Y.; Xu, X.C.; Chen, Z.H. Research on residual mechanical properties of post-fire 6061-T6 aluminum alloy extruded profiles. *Spat. Struct.* **2018**, *24*, 75–82. (In Chinese)
25. *GB/T 228.1-2010*; Metal Materials-Tensile Testing-Part 1: Method of Test at Room Temperature. China Standards Press: Beijing, China, 2010.